PUBLICATIONS OF THE ASTRONOMICAL SOCIETY OF THE PACIFIC, **121**:1395–1408, 2009 December

The Palomar Transient Factory: System Overview, Performance, and First Results

NICHOLAS M. LAW,[1] SHRINIVAS R. KULKARNI,[1] RICHARD G. DEKANY,[1] ERAN O. OFEK,[1] ROBERT M. QUIMBY,[1]
PETER E. NUGENT,[2] JASON SURACE,[3] CARL C. GRILLMAIR,[3] JOSHUA S. BLOOM,[4] MANSI M. KASLIWAL,[1]
LARS BILDSTEN,[5] TIM BROWN,[6] S. BRADLEY CENKO,[4] DAVID CIARDI,[3] ERNEST CRONER,[1]
S. GEORGE DJORGOVSKI,[1] JULIAN VAN EYKEN,[3] ALEXEI V. FILIPPENKO,[4] DEREK B. FOX,[7]
AVISHAY GAL-YAM,[8] DAVID HALE,[1] NOUHAD HAMAM,[3] GEORGE HELOU,[3]
JOHN HENNING,[1] D. ANDREW HOWELL,[6,9] JANET JACOBSEN,[2] RUSS LAHER,[3]
SEAN MATTINGLY,[3] DAN MCKENNA,[1] ANDREW PICKLES,[6] DOVI POZNANSKI,[2,4]
GUSTAVO RAHMER,[1] ARNE RAU,[1,10] WAYNE ROSING,[6] MICHAEL SHARA,[11]
ROGER SMITH,[1] DAN STARR,[4,6] MARK SULLIVAN,[12] VISWA VELUR,[1]
RICHARD WALTERS,[1] AND JEFF ZOLKOWER[1]

Received 2009 June 30; accepted 2009 September 29; published 2009 November 12

ABSTRACT. The Palomar Transient Factory (PTF) is a fully-automated, wide-field survey aimed at a systematic exploration of the optical transient sky. The transient survey is performed using a new 8.1 square degree camera installed on the 48 inch Samuel Oschin telescope at Palomar Observatory; colors and light curves for detected transients are obtained with the automated Palomar 60 inch telescope. PTF uses 80% of the 1.2 m and 50% of the 1.5 m telescope time. With an exposure of 60 s the survey reaches a depth of $m_{g'} \approx 21.3$ and $m_R \approx 20.6$ (5σ, median seeing). Four major experiments are planned for the five-year project: (1) a 5 day cadence supernova search; (2) a rapid transient search with cadences between 90 s and 1 day; (3) a search for eclipsing binaries and transiting planets in Orion; and (4) a 3π sr deep H-alpha survey. PTF provides automatic, real-time transient classification and follow-up, as well as a database including every source detected in each frame. This paper summarizes the PTF project, including several months of on-sky performance tests of the new survey camera, the observing plans, and the data reduction strategy. We conclude by detailing the first 51 PTF optical transient detections, found in commissioning data.

Online material: color figures

1. INTRODUCTION

The Palomar Transient Factory (PTF) is a comprehensive transient detection system including a wide-field survey camera, an automated realtime data reduction pipeline, a dedicated photometric follow-up telescope, and a full archive of all detected sources. The survey camera achieved first light on 2008 December 13; the project is planned to complete commissioning in 2009 June.

This paper describes the technical aspects of the PTF project. An accompanying paper (Rau et al. 2009) describes the science planned for PTF in detail; subsequent papers will discuss the various PTF pipelines in more detail as well as the results from the PTF surveys.

The transient detection survey component of PTF is performed at the automated Palomar Samuel Oschin 48 inch telescope (P48); candidate transients are photometrically followed up at the automated Palomar 60 inch telescope (P60). This dual-telescope approach allows both high survey throughput and a very flexible follow-up program.

[1] Caltech Optical Observatories, California Institute of Technology, Pasadena, CA 91125; nlaw@astro.caltech.edu.
[2] Lawrence Berkeley National Laboratory, Berkeley, CA 94720.
[3] Infrared Processing and Analysis Center, California Institute of Technology, Pasadena, CA 91125.
[4] Department of Astronomy, University of California, Berkeley, CA 94720-3411.
[5] Kavli Institute for Theoretical Physics and Department of Physics, University of California, Santa Barbara, CA 93106.
[6] Las Cumbres Observatory Global Telescope Network, 6740 Cortona Dr. Santa Barbara, CA 93117.
[7] Department of Astronomy and Astrophysics, Pennsylvania State University, University Park, PA 16802.
[8] Benoziyo Center for Astrophysics, Weizmann Institute of Science, 76100 Rehovot, Israel.
[9] Department of Physics, University of California, Santa Barbara, CA 93106.
[10] Max-Planck Institute for Extra-Terrestrial Physics, 85748 Garching, Germany.
[11] Department of Astrophysics, American Museum of Natural History, New York, NY 10024.
[12] Oxford Astrophysics, Department of Physics, Denys Wilkinson Building, Keble Road, Oxford, OX1 3RH, UK.

PTF's survey camera is based on the CFH12K mosaic camera formerly at the Canada-France-Hawaii Telescope, newly mounted on the P48 telescope at Palomar Observatory, California (and called "the PTF Survey Camera"). The camera has 101 megapixels, 1″ sampling and a 8.1 square degree field of view (FOV). Observations are mainly performed in one of two broadband filters (Mould-R, SDSS-g'). Under median seeing conditions (1.1″ at Palomar) the camera achieves 2.0″ FWHM images, and reaches 5σ limiting AB magnitudes of $m_{g'} \approx 21.3$ and $m_R \approx 20.6$ in 60 s exposures.

Data taken with the camera are transferred to two automated reduction pipelines (Fig. 1). A near–real-time image subtraction pipeline is run at Lawrence Berkeley National Laboratory (LBNL) and has the goal of identifying optical transients within minutes of images being taken. The output of this pipeline is sent to UC Berkeley where a source classifier determines a set of probabilistic statements about the scientific classification of the transients based on all available time-series and context data.

On timescales of a few days, the images are also ingested into a database at the Infrared Processing and Analysis Center (IPAC). Each incoming frame is calibrated and searched for objects, before the detections are merged into a database. This database will be made public after an 18 month proprietary period. Securely-classified transient detections will be publicly released on shorter timescales, depending on the details of the relevant projects (see Rau et al. 2009).

Follow up of detected transients is a vital component of successful transient surveys. The P60 photometric follow-up telescope automatically generates colors and light curves for interesting transients detected using P48. The PTF collaboration also leverages a further 15 telescopes for photometric and spectroscopic follow up. An automated system will collate detections from the Berkeley classification engine, make them available to the various follow-up facilities, coordinate the observations, and report on the results.

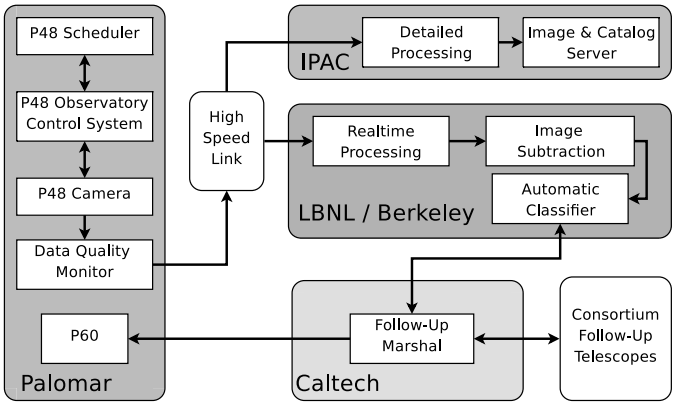

FIG. 1.—Overview of the PTF project data flow. See the electronic edition of the *PASP* for a color version of this figure.

This paper is organized as follows: in § 2 we describe the new PTF survey camera and automated observing system, and detail the on-sky performance of the system. Section 3 discusses the initial PTF observing strategy. Section 4 describes the automated data reduction pipeline and transient classification system, and § 5 details the PTF follow-up systems. In § 6 we conclude by describing PTF's first confirmed optical transient detections.

2. THE PTF SURVEY SYSTEM: P48+THE PTF SURVEY CAMERA

The P48 telescope is a wide-field Schmidt with a 48 inch aperture, a glass corrector plate, and a 72 inch (f/2.5) mirror (Harrington 1952). The telescope performed both Palomar Sky Surveys (POSS I and POSS II; Reid et al. 1991), and recently completed the Palomar-Quest digital synoptic sky survey (Djorgovski et al. 2008), before the start of PTF modifications in 2008 autumn.

The PTF survey camera (Fig. 2) is based on the CFH12K camera (Cuillandre et al. 2000). The camera was extensively re-engineered by Caltech Optical Observatories for faster readout, closed-cycle thermal control, and robust survey operation. The CCD focal plane was untouched but the rest of the camera was modified for reliable and low-cost operation on the P48. Primary requirements for the design, in addition to the mechanical and optical modifications required for operation on P48, were to reduce the operation cost of the camera, to minimize the beam obstruction, and to increase the readout speed for PTF operations.

The P48 telescope optics are significantly faster than the CFHT, leading to stringent requirements on the camera's CCD array flatness and optical quality. The low operation cost requirement led to swapping the camera cooling system from a LN_2 system to a CryoTiger closed-cycle cooler. The camera was also upgraded with a new precision shutter and filter-changer assembly. The telescope was refurbished for operation with PTF and a new queue-scheduling automated observatory control system was implemented.

We summarize here the upgrades and provide on-sky performance test results for the PTF survey camera on P48; more detail on the camera engineering is provided in Rahmer et al. (2008). Table 1 summarizes the survey and P60 follow-up system specifications.

2.1. CCD Array

The core of the PTF survey camera is a $12\text{K} \times 8\text{K}$ mosaic made up of 12 $2\text{K} \times 4\text{K}$ MIT/LL CCID20 CCDs, arranged in a 6×2 array (Fig. 3). Three of the CCDs are high-resistivity bulk silicon (HiRho); the rest are standard epitaxial silicon (EPI). The EPI chips reach QEs of approximately 70% at 650 nm; the HiRho devices have somewhat higher QE, reaching

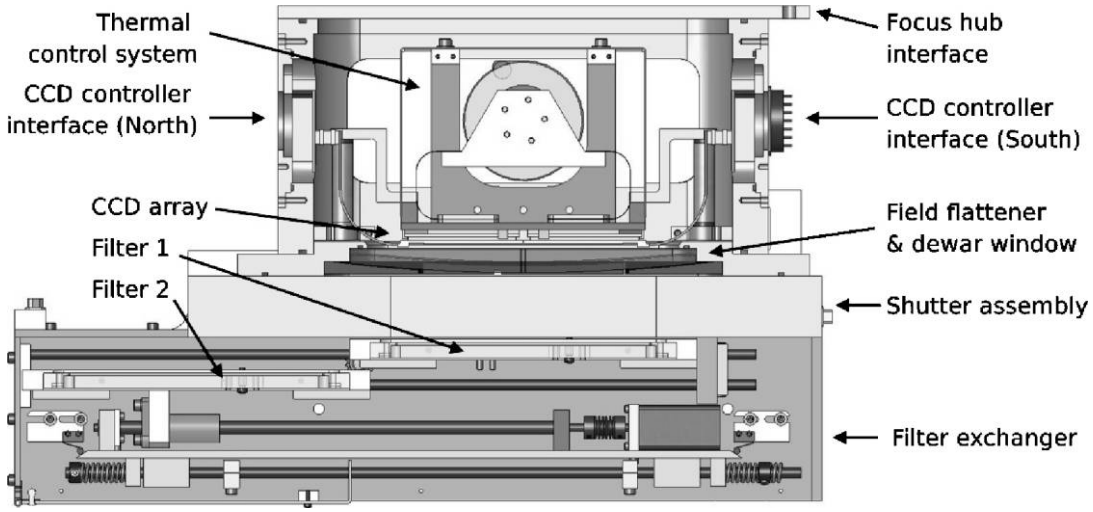

FIG. 2.—Cut-away diagram of the PTF survey camera after modifications for use on the Palomar 48 inch telescope. The diagram is orientated so downwards is in the direction of the P48 primary mirror when mounted in the telescope. From bottom up, the components are: the filter exchanger, shutter, and the dewar assembly including the CCD window and CCD array. See the electronic edition of the *PASP* for a color version of this figure.

$\approx 90\%$ at 650 nm (Fig. 4). The HiRho chips also have lower fringing levels due to their increased thickness.

Depth of focus, and thus the flatness of the CCD array, is an important issue for the P48's f/2.5 beam. Approximately 92% of the PTF survey camera's CCD array is within 20μm of the reference focal plane position. Taking a detailed error budget into account, including terms for telescope jitter, atmospheric turbulence, and the optical quality, we predicted that 89% of the array would provide images meeting our 2.0″ FWHM image quality budget and that the remainder of the array would be within 0.2″ of the specification. On-sky tests confirm this (§ 2.9; the best images so far taken have a median FWHM of 1.5″ across the array). The instrument tip and tilt was adjusted to better than 0.003° tilt across the entire array using 20μm shims at the dewar mounting points and on-sky image tilt measurements from FWHM maps. The final full field-of-view image quality is better than 2.0″ FWHM in median seeing (§ 2.9).

The CCDs are 3-edge buttable and are separated by gaps of $\approx 500\mu$m, corresponding to 35″ (see Fig. 3 for more details). The CCD array itself has a low number of bad pixels and offers excellent image quality across the field of view (Fig. 5).

The full CCD array readout time is 30.7 s, using independent amplifiers for each chip and two Generation 3 Leach (SDSU) devices reading out 6 CCDs each. This readout time is approximately half that of the original camera electronics and was specified to match the expected telescope slew and settle time for PTF operations. The improved speed was reached at a small cost in readout noise; even so the final readout noise is $<15\ e^-$ on all chips, well below the expected sky noise.

During the camera upgrade process, CCD03 became unresponsive. After diagnosing the fault as a problem inside the CCD package itself, we decided that attempting to repair the CCD would be both an unacceptable risk to the array and an unacceptable delay to the project. We are continuing to evaluate ways to repair or replace the malfunctioning CCD, but for at least the first year of science operations, PTF is accepting the 8% loss of imaging area.

2.2. Optics

We replaced the original flat dewar window with a field-flattening optic designed for P48's curved focal plane. The new optics are designed to provide better than 2″ image quality over the entire 3.4° span of the image in median seeing, including atmospheric, optical and mechanical tracking error terms. The optical distortion is 0.11% at the corners of the array relative to a uniform grid, a level comparable to differential atmospheric refraction over our field of view (Fig. 6 shows the distortion field).

The telescope optics were also optimized: the primary mirror supports were tuned; all optical surfaces were cleaned or refurbished; baffles were improved to control stray light; the telescope tube was rendered light tight; and internal stabilized calibration sources were added to allow daytime quality control.

2.3. Cooling System

The original liquid nitrogen cooling system was replaced with a closed-cycle cooling system, implemented via a compact cold head located close to the CCDs. A Polycold Compact Cooler (formerly known as CryoTiger) with an expansion head with no moving parts was chosen to minimize vibration. We attached an H-shaped copper head spreader to the cold head to provide a nearly isothermal surface to which to attach flexible copper heat exchange straps leading to the CCD array assembly.

TABLE 1
SPECIFICATIONS OF THE PTF SURVEY SYSTEM

P48 Survey Characteristics	
Telescope	Palomar 48 inch (1.2 m) Samuel Oschin
Camera field dimensions	$3.50° \times 2.31°$
Camera field of view	8.07 square degrees
Light-sensitive area	7.26 square degrees
Plate scale	$1.01''$ pixel^{-1}
Efficiency	66% open shutter (slew during readout)
Sensitivity (median)	$m_R \approx 20.6$ in 60 s, 5σ
	$m_{g'} \approx 21.3$ in 60 s, 5σ
Image quality	2.0 arcsec FWHM in median seeing
Filters	g' & Mould-R; other bands available
P48 Survey Camera CCD Array	
Component CCDs	12 CCDs; 1 nonfunctional
CCD specs	2K $\times$ 4K MIT/LL 3-edge butted CCDs
Array leveling	Flat to within 20μm
Pixels	$15\mu m$ pixel^{-1}; 100% filling factor
Chip gaps	Median 35 pixels (35″)
Readout noise	<20 e^-
Readout speed	30 s, entire 100 megapixel array
Gain	1.6 e^-ADU^{-1} (typical)
Linearity	Better than 0.5% up to 60 K ADUs
Optical distortion	Maximum 7″ at array corners compared to flat grid
P60 Follow-up Camera Specifications	
Telescope	Palomar Observatory 60 inch (1.5 m)
CCD specs	2K $\times$ 2K CCD
Plate scale	$0.38''$pixel^{-1}
Readout noise	5 e^- (amp 1); 8 e^- (amp 2)
Gain	2.2 e^- ADU^{-1} (amp 1)
	2.8 e^- ADU^{-1} (amp 2)
Readout speed	25 s (full frame)
Linearity	Better than 1% up to 20 K ADUs
Sensitivity (median)	$m'_g \approx 21.6$ in 120 s, 5σ
	$m_{r'} \approx 21.3$ in 120 s, 5σ
	$m_{i'} \approx 21.1$ in 120 s, 5σ
	$m_{z'} \approx 20.0$ in 120 s, 5σ

A heating system attached to the dewar window actively maintains the CCD array temperature at 175 K.

2.4. Shutter

The shutter is a commercial unit supplied by Scientific Instrument Technology, and employs dual split blades to avoid beam obscuration by the blades when the shutter is open. Only one blade covers the CCD array at any one time. An exposure sequence consists of stowing one blade, thus uncovering the CCD array, and then after an interval moving the second blade to cover the CCD array. The sequence is repeated in the opposite direction for the next exposure. The shutter unit is designed to provide minimal vignetting, and a frame-to-frame variation in exposure time of less than 2 ms, for all parts of the CCD array. The blade transit time is 1.300 s but the blades can be independently controlled to allow shorter exposure times in a slit scanning across the detector.

2.5. Filter Changer

The filter changer assembly is a custom-built mechanism that provides for motorized selection of one of two filters; one filter is always in the field. Filter exchanges are completed in 15 s, using a microstepper motor. Absolute filter positioning is registered by running the filter frame against a mechanical hard stop. Normal PTF operation is expected to use at most two filters in each night, but the system has been designed for easy manual swapping of filters as necessary.

2.6. Camera Electronics and Software

The PTF survey camera array of 12 CCDs is divided into two banks of six CCDs, with each bank handled separately by its own detector controller. The controllers are Generation 3 Leach (SDSU) devices comprised of three 2 channel video boards, three clock boards, and a timing board. Communication between a controller and its respective host computer is

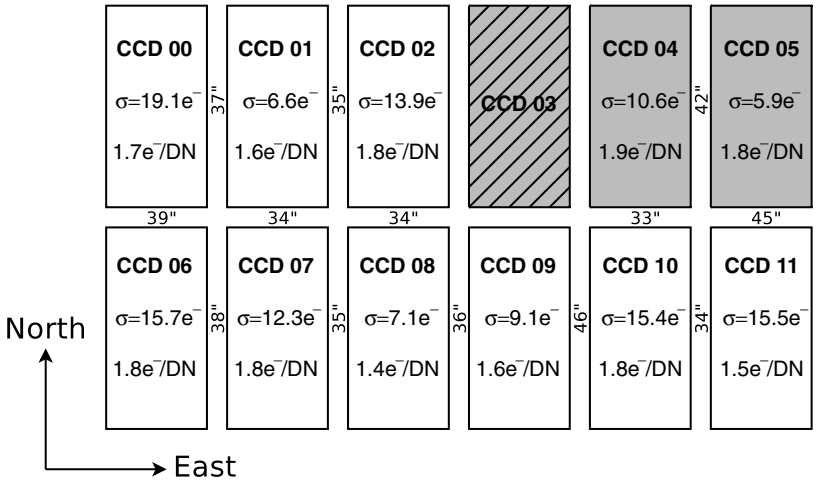

FIG. 3.—Schematic of the PTF survey camera focal plane (with greatly expanded chip gaps). The HiRho chips (*shaded*) are high-resistivity silicon with improved red quantum efficiency (Fig. 4). The read noise and gain is noted for each chip; some chips show relatively high read noise and are being optimized in ongoing work. CCD03 is unresponsive and will be replaced later in the PTF project. Chip gaps are noted in arcseconds, based on on-sky astrometric solutions.

conducted via a fiber optic serial link between the timing board and a corresponding PCI card in the host computer. The controllers share a common clock so that the exposures and readouts of the two controllers are synchronized with each other. The master camera computer also handles all the nondetector camera hardware—the shutter, filter changer, temperature sensors, and calibration LEDs. The camera control software is custom built for the PTF survey camera, and is based on panVIEW, the Pixel Acquisition Node (PAN) version of ArcVIEW (Ashe et al. 2002).

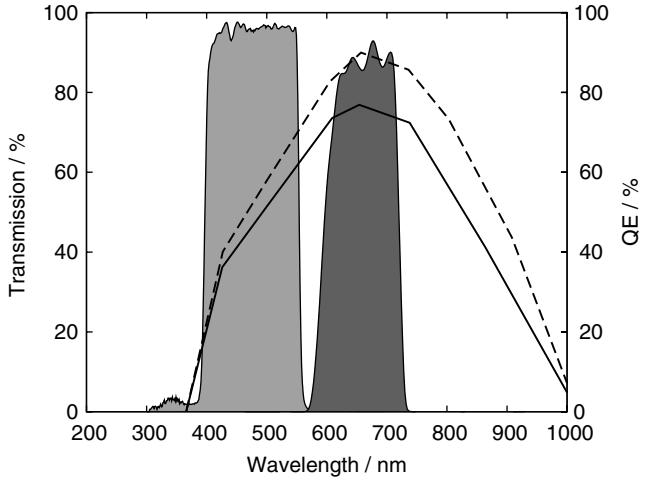

FIG. 4.—The quantum efficiencies of the nine EPI chips in the CCD array (*solid line*) and the three HiRho chips (*dashed line*). Filter transmission curves for the two primary PTF survey filters are also shown (*filled curves*; *left,* SDSS-g'; *right,* Mould-R). The QE curves and Mould-R transmission are adapted from Cuillandre et al. (2000). See the electronic edition of the *PASP* for a color version of this figure.

2.7. PTF Observatory Control System and Scheduler

The survey operations are performed robotically by the P48 Observatory Control System (OCS), written in MATLAB. The OCS is responsible for controlling the camera, filter exchanger, shutter, telescope, dome, and focuser, on the basis of feedback information from the scheduling system, the camera and telescope, a weather station, and the data quality monitor (§ 2.8).

The OCS is responsible for sequencing all PTF observations, starting with the bias frames before sunset, through focus images, and finally the science images. The PTF scheduler is responsible for selecting the next target for observation. The PTF schedule is not predefined; the next target is selected 30–90 s before each exposure starts, during the previous exposure.

The criteria for selection of the next target include: (1) Sun altitude; (2) excess in sky brightness due to the Moon, using the algorithm of Krisciunas & Schaefer (1991); (3) Moon phase; (4) time needed to move telescope to the next target; (5) time needed to move dome to the next target; (6) airmass; and (7) time since the last sequence of observations of this field. In addition for some programs, such as the 5 day cadences (§ 3.2), the scheduler is required to optimize the field selection so that each field is observed twice during the night for asteroid detection.

These criteria are used to calculate weights for each field, and the scheduler selects the target with the highest weight for observation. In order to keep the operations of the scheduler as simple as possible, most of the weights follow a step function. An exception is the cadence (time since last observation) weight (W) which is of the form

$$W = 1 - \frac{1}{1 + \exp\{[(\mathrm{JD} - \mathrm{JD}_l) - \tau]/s\}} \qquad (1)$$

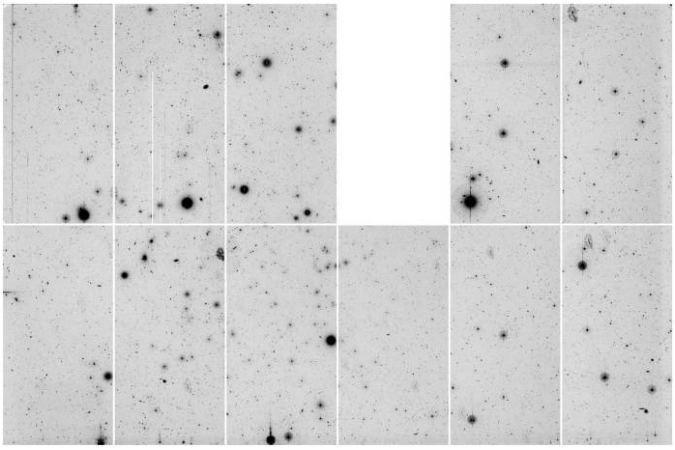

FIG. 5.—A typical R-band image taken with the PTF survey camera on the Palomar 48 inch telescope, with the same orientation as Fig. 3. The image has been bias corrected and flat fielded but, to show the cosmetic quality of each chip, no dithering has been applied.

where JD is the current Julian day, JD_l is the Julian day corresponding to the last successful sequence (pair of images) of observation, τ is the cadence, and s is a softening parameter that defines the time scale in which the weight goes from near 0 to near 1.

2.8. Data Quality Monitoring

A software suite running at the mountain, the Data Quality Monitor (DQM), analyzes all the recorded images as they are taken. An initial check searches for problems with file corruption, truncation, or missing FITS headers. Next, the image is searched for stellar objects (using SExtractor; Bertin & Arnouts 1996), and the average FHWM and other image quality parameters are checked for obvious problems. Finally, if it has passed all the checks, the file is sent to the PTF pipelines.

To detect more subtle image quality problems such as increased electronic noise, the P48 twice daily automatically takes test exposures of the telescope tube cover. A band of temperature-stabilized LEDs provides illumination stable to $<0.1\%$. Because the illumination has passed through every optical element of the system, comparing the test exposures to reference exposures provides a simple test if anything in the telescope + camera + electronics systems is not operating as expected. Many problems can be found and corrected before the start of nighttime operations.

Finally, both the LNBL and IPAC pipelines produce image quality and sensitivity measures for all detected fields, providing a long-term monitoring facility to allow us to optimize our observing setup and equipment.

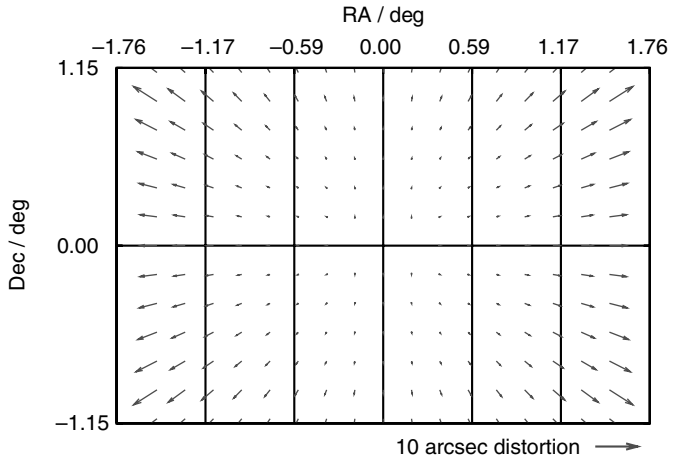

FIG. 6.—Distortion map across the PTF survey camera focal plane, relative to a flat grid on the sky and based on Zemax modeling of the optical system. A 10″ distortion scale is indicated at the bottom of the figure. The maximum distortion at the corners of the CCD array is 7″, or 0.11%. See the electronic edition of the *PASP* for a color version of this figure.

2.9. On-Sky Performance

The PTF survey camera system achieved first light on 2008 December 13. Initial commissioning work was completed in 2009 January and the system has been used for initial science test operations since then (with small gaps for engineering). Here we describe on-sky performance results from the first 2 months of operation. Since the system continued to be commissioned during this time, the performance is likely to improve as the PTF survey continues.

A total of 91.7% of the pixels in the full $12\mathrm{K} \times 8\mathrm{K}$ array are light sensitive and not dark, occulted, or otherwise bad (this increases to $>99\%$ good pixels if we exclude the unresponsive CCD). Most of the approximately 200 bad columns in the array are concentrated on CCD05 (at one corner of the field). CCD09 offers the best combination of PSF quality and CCD cosmetics. The chips are linear to better than 0.5% up to 60,000 ADUs (typical gain is 1.6 e^- ADU^{-1}).

During the design of the PTF survey camera we specified a FWHM of 2.0″ during median Palomar conditions (1.1″ seeing). This requirement was based on a number of factors—the minimum PSF size that is reasonably sampled by our 1″pixel^{-1} plate scale; what could be reasonably achieved with the P48 optical setup; optimization of the survey limiting depth; and the requirement to detect supernovae in the cores of bright nearby galaxies. Analysis of the first two months of PTF on-sky data shows that we have met or exceeded this requirement. Typical images taken in good seeing show both sub-2.0″ FWHMs and very small variations in image quality across the entire field of view (Figs. 7 and 8).

The survey depth is correspondingly encouraging (as shown in Fig. 9). Based on all the data taken during the last 2 months of commissioning, the system provides median 5σ, 60 s limiting dark-time magnitudes of $m_{g'} = 21.3$ (25th percentile $m_{g'} = 21.7$; 75th percentile $m_{g'} = 21.0$) and $m_R = 20.6$ (25th percentile $m_R = 20.8$; 75th percentile $m_R = 20.3$).

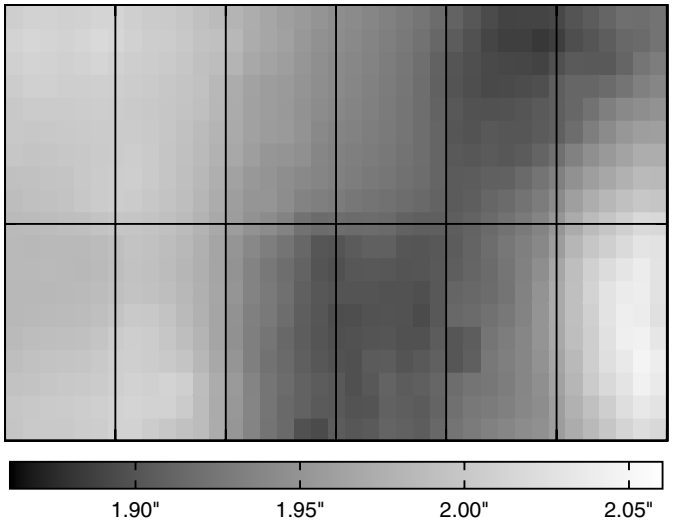

FIG. 7.—A map of the FWHM variations across the PTF survey camera focal plane array from a typical R-band observation (with the same orientation as Fig. 3). Image FWHM measurements are interpolated over the unresponsive CCD for ease of interpretation. The residual FWHM variations are on the order of 0.2″ and are due to the 20 μm flatness of the CCD array and slightly decreasing optical performance at the edge of the field of view.

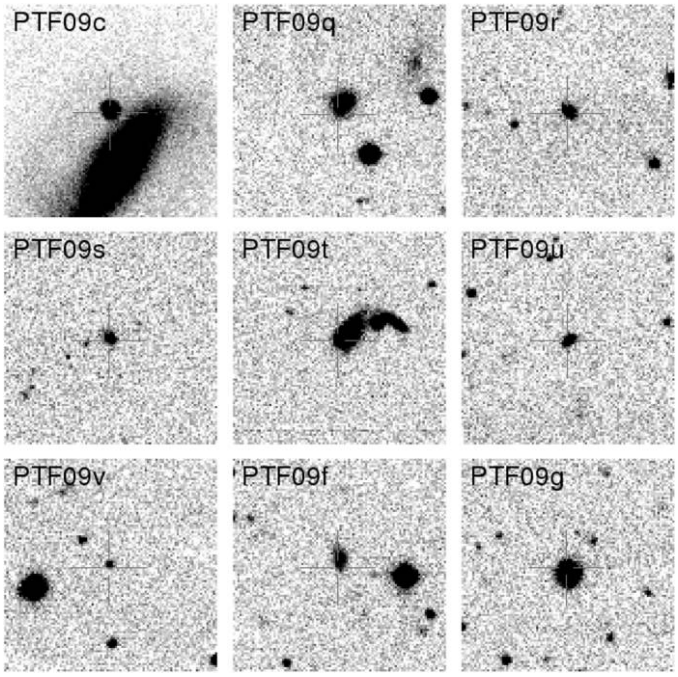

FIG. 8.—100″ cutouts from R-band PTF survey camera images, from the first set of PTF optical transient detections. *Crosshairs* show the transient detection position, most inside galaxies. The properties of the detected transients are given in § 6, with the exception of PTF09c, which is a rediscovery of SN 2009an. The images are distributed widely across the focal plane. See the electronic edition of the *PASP* for a color version of this figure.

The entire PTF survey system (the P48 telescope, PTF survey camera, OCS, and the DQM) has a current uptime of $\approx 90\%$, excluding losses due to weather. As initial science operations proceed, many issues are being addressed and the uptime is continually improving. The survey efficiency is currently approximately 50% open-shutter time, compared to a goal (and theoretical maximum) of 66%. This is due to the cumulative effect of many small inefficiencies in the system operation and is continually improving.

3. THE PTF OBSERVING STRATEGY

PTF will pursue four distinct experiments optimized for different times of the year. Each project is designed to use P48 only as the survey telescope while other PTF resources are reserved for follow-up observations. We here describe the observing strategy for each of the major PTF experiments; Rau et al. (2009) give a detailed discussion of the science planned for each project. The experiments are summarized in Table 2.

3.1. Observing Setup and Filter Selection

The three major PTF experiments, together accounting for 92% of the project's P48 time, are based on two filters: SDSS g' and Mould-R (Fig. 4). These filters were chosen to optimize the survey detection limits in full moon (R-band) and dark-sky (g'-band) conditions for a variety of different transient classes (see Rau et al. 2009). During dark-sky conditions, the reduced quantum efficiency in the g' filter is more than compensated for by the darker sky and the blue colors of many of our targeted transients. Mould-R is very similar to SDSS r' and allowed us to reuse an existing CFH12K filter; it is the standard filter for programs that are expected to spend at least part of their time operating while significant moonlight is present. Because no follow-up is done with P48, we elected to use standard passbands for the survey to allow a meaningful comparison of PTF detection magnitudes to follow-up telescope results.

The initial standard exposure time for the 5DC and DyC surveys is 60 s, based on the readout time of the camera, expected system efficiency, and the expected sky noise and dark current in the exposures. In later stages of the PTF project this exposure time will be optimized for the different programs expected to be pursued.

3.2. 5 Day Cadence

The 5 day cadence experiment (5DC) will run yearly from March 2 until October 30 using 65% of the time in that period. The main goal of this experiment is to construct large samples of type-Ia SNe and core-collapse SNe. It will also study AGNs, quasars, blazars, CVs, extragalactic novae, luminous red novae, and tip of the AGB variability. The experiment will observe a footprint of approximately 8000 square degrees, with $|b| > 30°$, ecliptic latitude $|\beta| > 10°$, and with a median cadence of 5 days. At a given time, the active area for the 5DC search (including all

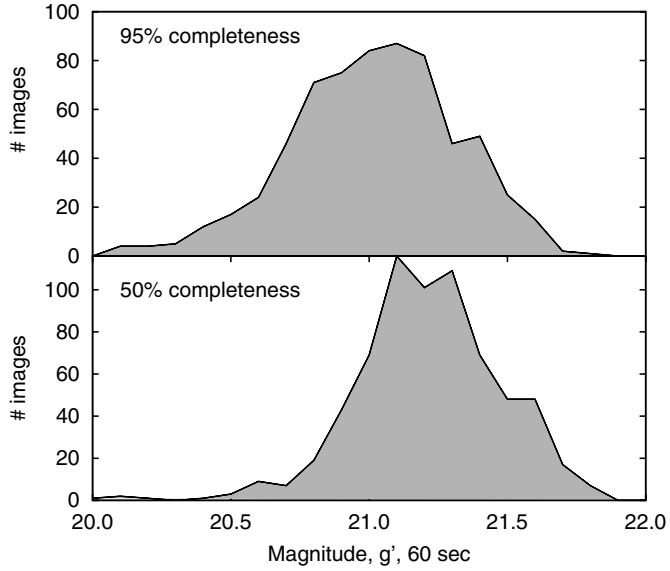

FIG. 9.—Completeness limits from a typical g' band, photometric, PTF survey night. Each curve represents the minimum detectable magnitude at either 50% or 95% completeness; each exposure of each chip is treated as an individual image. The spread in values arises from variations due to seeing, the imaging quality of each chip and the airmass of the observations, and thus represents typical performance for the actual PTF observation strategy.

overheads) will be 2700 square degrees. The 5DC observations will be conducted in almost all lunar phases in R band. In each epoch we will obtain two 60 s exposures separated by 60 minutes. The two images will be used to remove cosmetic artifacts and cosmic rays and to find solar system objects.

3.3. Dynamic Cadence

The dynamic cadence experiment (DyC) is designed to explore transient phenomena on time scales shorter than ~5 days and longer than 1 minute. The experiment will explore unknown territories in the transients phase space—mainly fast transients with time scales of less than a day. Therefore, the dynamic cadence will be an evolving experiment. Every 6 months, the PTF collaboration will review the results of the dynamic cadence experiment and decide how to continue.

Motivated by a search for short-lived transients in the brightness gap between novae and supernovae ($-10 < M < -16$), the DyC experiment is targeted at fields that are luminosity concentrations in the local universe. Since these transients are expected to be fainter than $M \sim -16$, the search volume is limited to DM (distance modulus) <36.5, i.e., less than 200 Mpc.

The total luminosity of nearby galaxies in the PTF FoV was computed on a fine grid of possible pointings (limited by declination > -30). This was done 7 times with 7 different maximum distances (in steps of 0.5 between $30.5 \leq \mathrm{DM} \leq 36.5$). We assigned a weight for each pointing based on the fraction of maximum luminosity in that list. A total weight for each pointing was computed by averaging the individual weights. Finally, pointings with the highest weights were chosen for PTF. This list naturally includes the nearest, brightest galaxies (e.g., M31, M51, M81) and nearest galaxy clusters (e.g., Virgo, Perseus, Coma), but also covers the other accessible nearby mass concentrations from physical and chance galaxy alignments.

This experiment will detect RR Lyr stars in the Galactic halo, CVs, AM CVn stars, flare stars, SNe, eclipsing binaries, and solar system objects. Moreover, this experiment will put strong constraints on the existence of any optical counterparts that may be associated with radio transients.

3.4. Orion Field

The Orion project has been assigned 40 consecutive nights year^{-1} for 3 yr to perform intensive time-series observations of a single field in the Orion star forming region, with the aim of detecting close-in Jupiter-sized planets transiting young stars. The observations will be acquired in R band with no dithering in a continuous sequence of 30 s images, with the goal of producing high-precision (better than 1%) differential photometry. The field will be chosen to represent a stellar age range where protostellar disks should be on the point of dissipation (5–10 Myr)—giving important clues about planet formation and migration—and to optimize for source density and avoid regions where the stellar variability in the ensemble is severe enough to prohibit precise differential photometry. The IPAC PTF pipeline will be used for standard image reduction, source identification, and astrometry, but a dedicated photometric pipeline is being developed to produce the high-precision differential photometry.

3.5. Deep Hα Sky Survey

For 3 nights each lunation during full Moon we will carry out a 3π sr sky survey in Hα. The survey area will include all the sky

TABLE 2
PTF EXPERIMENTS PLANNED FOR THE FIRST YEAR OF OPERATIONS

Experiment	% of Total	Cadences	Filter	Months
5 day cadence (5DC)	41	5 days	R	Mar-Oct
Dynamic cadence (DyC)	40	1 minute–5 days	g', R	All year
Orion	11	1 minute	R	Nov-Jan
Hα	8		Hα	All year

with $\delta > -25°$. Each field will be observed twice in four narrowband (approximately 10 nm width) filters around the Hα line covering the redshift range of about zero to 0.05, corresponding to distances of 0 to 200 Mpc. Narrowband filters that give a consistent bandpass across the entire field of view of the camera are difficult to produce, especially in the fast beam of the P48. However, a description of usable Hα filters for a Schmidt telescope with the same optical design is given in Parker & Bland-Hawthorn (1998), and our industrial partners are confident that these filters can be constructed.

We estimate that the Hα survey sensitivity limit will be $\approx 0.6R$ in a 2.5″ aperture[13]; a detailed comparison of this sensitivity to other Hα surveys can be found in Rau et al. (2009). We are currently designing a scheme that will allow us to photometrically calibrate these data to about 10% accuracy.

4. DATA REDUCTION AND TRANSIENT DETECTION

All PTF data taken at P48 is automatically routed to two pipelines: a realtime transient detection pipeline, optimized for rapid detection of interesting objects, and a longer-term archival pipeline optimized for high-precision and easy searching of the results.

4.1. Realtime Transient Detection

The PTF quick-reduction and subtraction pipeline was designed from the start to take full advantage of the parallel high performance computing facilities at the National Energy Research Scientific Computing Center (NERSC).[14] The major improvement to the hardware used in this pipeline over previous versions designed by the Supernovae Cosmology Project (Perlmutter et al. 1999) and Nearby Supernovae Factory (Aldering et al. 2002) at LBNL is the use of the NERSC Global Filesystem (NGF). NGF is a 300 terabyte shared file system with over 1 gigabyte s^{-1} bandwidth for streaming I/O which can be seen by all of the high-performance computers. On the software front, the improvements include a tight coupling of a PostgreSQL database involved in tracking every facet of the image processing, reference building, image subtraction and candidate detection along with a complete rewrite of the processing and subtraction codes, described as follows.

Incoming P48 images are immediately backed up on the High Performance Storage System, a 3 petabyte tape archive system at NERSC. Processing begins by splitting the packed images apart by chip, applying crosstalk corrections, and performing standard bias/overscan subtraction and flatfielding. After this point, all operations are performed on a chip-by-chip basis in parallel. Catalogs of sources are created for each image via the Terapix SExtractor code (Bertin & Arnouts 1996), which then is fed to the astrometry.net[15] code to perform an astrometric solution. At this point a comparison to the USNO-B1 (Monet et al. 2003) catalog is made to determine the zeropoint and 3σ limiting magnitude of the image along with a calculation of the seeing. The image is then loaded into the processed image database, storing all relevant information from the FITS headers.

After several images are obtained for a given PTF pointing, we are able to create a reference image. The reference images are created via the Terapix software Scamp and Swarp (Bertin 2006) after querying the processed image database in order to obtain the highest quality input images for a given pointing/chip combination. The references are assigned version numbers and (along with their relevant information) are stored in the reference database.

Subsequent new images are processed as just described, and if a reference image exists for them, a subtraction is performed. First, the new image is astrometrically aligned to the reference by utilizing Scamp and the new and reference catalogs. The reference is then Swarped to the size and scale of the new image and a subtraction is performed using HOTPAnTS[16]. The subtraction is performed in both the positive and negative direction (reference minus new and new minus reference) to detect both positive and negative flux changes. Candidate transient sources are detected via SExtractor and along with other relevant parameters (location with respect to bad pixels, etc.) are stored in a candidate and subtraction database. The subtraction image that led to the first PTF supernova discovery is shown in Figure 10.

In addition, PTF takes advantage of DeepSky.[17] DeepSky was started in response to the needs of several astrophysics projects hosted at NERSC. It is a repository of digital images taken with the point-and-stare observations by the Palomar-QUEST Consortium (Djorgovski et al. 2008) and the Near Earth Asteroid Team (Bambery et al. 2007). This data spans nine years and more than 15,000 square degrees, with 20–200 pointings on a particular part of the sky and cadences from minutes to years. For a large fraction of the survey, DeepSky achieves depths of $m_R > 23$ magnitude. In total there are more than 11 million images in DeepSky. This historical data set complements the Palomar Transient Factory survey by identifying known variable stars, AGN, and the detection of low surface-brightness host galaxies of supernovae.

During commissioning, human scanners were utilized to reject "junk" transient detections via a web interface. The subtraction system and rejection algorithms are currently being improved with an aim of full automation by making use of machine learning techniques. The results of human scanners

[13] R is a unit of surface brightness commonly used in aeronomy. One R (one Rayleigh) is $106/(4\pi)$ photons $cm^{-2}\ s^{-1}\ sr^{-1}$. For the Hα line the intensity in cgs units is 2.41×10^{-7} erg $cm^{-2}\ s^{-1}\ sr^{-1}$.

[14] See http://www.nersc.gov.

[15] At http://astrometry.net.

[16] See http://www.astro.washington.edu/users/becker/hotpants.html.

[17] At http://www.deepskyproject.org.

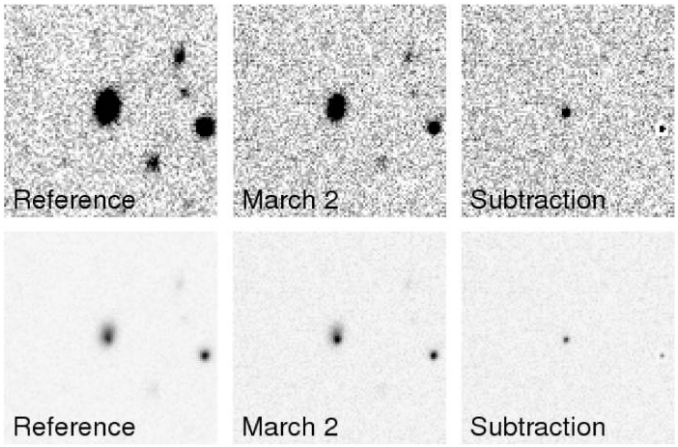

FIG. 10.—The detection images of SN 2009av, PTF's first confirmed transient detection. The top and bottom row show the same images at different stretches.

are being used to train an automatic classifier; a more detailed account of this classification technique is in preparation.

Any statistical inference of PTF transient rates will require a careful measurement of the survey detection efficiency. We have constructed a pipeline that produces realistic fake variable objects and adds them into PTF images, on which we apply the standard PTF search algorithms to determine the detection efficiency for any specific data subset. We currently model three generic classes of transients: variable stars, SN/AGN-like sources (i.e., point sources in host galaxies), and "rogue" transients (point sources on random positions in the image). The transients are directly injected into PTF images using point-spread functions (PSFs) modeled from nearby stars in the fields.

4.2. Realtime Automated Transient Classification

The Transients Classification Pipeline (TCP; Bloom et al. 2008; Starr et al. 2008a,2008b) is a parallelized, Python-based framework created to identify and classify transient sources in the real-time PTF differencing pipeline (§ 4.1). The TCP polls the candidate database from that pipeline and retrieves all available metadata about recently extracted sources. Using the locations and uncertainties of the transient candidate objects, the TCP either associates an object with existing known sources in the TCP database or, after passing several filters to exclude nonstellar (e.g., known minor planets) and nonastrophysical events, generates a new source. The Bayesian framework for event clustering is given in Bloom et al. (2008). Another classification engine will also be used on PTF transients (Mahabal et al. 2008a,2008b).

Once a transient source has been identified, the TCP generates "features" which map contextual and time-domain properties to a large dimensional real-number space. After generating a set of features for a transient source candidate, the TCP then applies several science classification tools to determine the most likely science class of that source. For rapid-response transient science, a subset of features—such as those related to rise times and the distance to nearby galaxies—is most useful. As light curves are better sampled and colors are obtained, more features are used in the classification. The resulting science class probabilities are stored in a database for further data-mining applications. Sources with high probabilities of belonging to a science class of interest to the PTF group will be broadcast to the PTF's "Follow-up Marshal" (§ 5) for scheduling of follow-up observations. As more observations are made for a known source, the TCP will autonomously regenerate features and potentially reclassify that source.

4.3. The IPAC PTF Image Processing Pipeline and Data Archive

While the transient pipeline will be optimized for rapid turnaround, the IPAC pipeline will be geared toward providing the best possible photometry consistent with hardware capabilities and data rate. To enable the generation of optimal calibration files (primarily flat fields), the IPAC pipeline will commence image processing only after all of a given night's observations have been received. Additional source association operations, database updates, and data transfer to the Infrared Science Archive (IRSA)[18] will be carried out over a period of several days. Processed images and incremental source lists will be available through IRSA within 2 days from the time the observations are taken.

After a given night's observations have been completed and received at IPAC (as indicated by receipt of end-of-night image manifest), the image processing pipeline is initiated. Parallel processing on 11 multiprocessor Linux machines is employed to simultaneously process the PTF mosaic's 11 working detectors and meet the data rate requirement. Key pipeline-processes are multithreaded to take full advantage of the 8 core CPU in each of the Linux machines.

The pipeline initially generates night-specific bias frames, and trims and bias-subtracts all images in the usual manner. Nightly flat fields are generated for each detector by source-masking and median-combining all of the night's sky observations; although twilight flats are taken each night, PTF data reductions use by preference these "superflats" generated from the night's observations. This is an involved and memory-intensive process and, given the number of exposures involved, takes 3–4 hr with the processing hardware currently in place. On completion, these flat fields are used to process the entire night's science observations. Raw and processed images as well as all ancillary and calibration frames are subsequently passed to IRSA for archiving and retrieval on demand.

Source detection is carried out using SExtractor (Bertin & Arnouts 1996). SExtractor is applied to each image a number

[18] See http://irsa.ipac.caltech.edu.

of times in the pipeline to mask sources prior to flat-field generation, measure the effective seeing, generate pixel weights and masks, and finally to generate photometry for all detected sources. Pixel masks are generated to flag bad rows and columns, cosmic rays, saturated pixels, and charge bleeding. The final application of SExtractor is carried out after multiplying the processed image by a pixel area map to preserve point-source photometry.

For each image, the SExtractor output list is then astrometrically calibrated using the Terapix Scamp software (Bertin 2006). Photometric zeropoints are determined by calibrating against stars in the Sloan Digital Sky Survey (York et al. 2000), taking color terms into account. With appropriate airmass corrections, these zeropoints are then applied to all sources outside the SDSS footprint. Ultimately photometric calibration may also be related to flux measures from (saturated) Tycho stars (Ofek 2008).

Currently in development is a source association pipeline that will match, on a nightly basis, each detected source with all previous detections of that source. Appropriate pointers will be incorporated into the IRSA database, enabling users to query the photometric time history of every object ever detected by PTF.

5. FOLLOWING-UP DETECTED TRANSIENTS

The automated Palomar 60 inch is the primary workhorse for photometric follow-up of PTF transients. Further photometric and spectroscopic characterization is performed on a worldwide network of other telescopes, including the Palomar Hale Telescope, the Keck telescopes, PARITEL, and the LCOGT telescope network.

5.1. Photometric Follow-up with P60

The automated P60 observation queue (Cenko et al. 2006) is sent all candidates flagged as bona fide astrophysical transients (i.e., a new point source detected at least twice in P48 imaging and which either lacks a counterpart or has a galaxy host in the reference imaging). A 120 s snapshot in g', r', i', z' is obtained for quick classification. On a typical night with median weather conditions, this reaches a limiting magnitude of $m'_g \approx 21.4$, $m'_r \approx 21.2$, $m'_i \approx 20.9$, and $m'_z \approx 19.8$. Our efficiency currently allows 20 2 minute exposures hr^{-1}.

As soon as the 60 inch data are obtained, an automated pipeline detrends the data and solves for an astrometric and zeropoint solution. Next, if the location is in SDSS, the pipeline downloads the corresponding SDSS image (mosaiced to fit the P60 FOV) to serve as a template. A convolution kernel is measured and image subtraction performed. On the subtracted image, PSF photometry is used to measure the magnitude at the source location and the result is sent to the PTF database. If the source is not detected, an upper limit is returned. Currently, if the location is outside SDSS, direct photometry is performed. We note that host galaxy light can be a significant contaminant which is not properly corrected for in case of direct photometry. Hence, even for fields outside SDSS, we are investigating other options for template imaging for image subtraction.

The 60 inch snapshot observation provides independent confirmation that the candidate is a real transient (and not a subtraction artifact), a color for quick classification (for example, $m_g - m_r \approx 0$ suggests that it is a SN Ia), and a second-epoch magnitude to assess photometric evolution. All this information helps direct further spectroscopic and multiband photometric follow-up with P60 and other telescopes.

5.2. The Follow-up Marshal

We have designed a centralized follow-up Marshal to ensure that our discoveries are efficiently distributed to our follow-up resources and that the temporal coverage of a given target meets the requirements of the appropriate science program. The design of this system is complete, but the automated follow-up program has not yet begun. A later paper will detail the performance of this novel system.

The first duty of the follow-up Marshal will be to monitor the output of the transient classifier to identify any new sources detected by P48 that warrant follow-up observations. For this purpose, the Marshal will maintain a list of target descriptions (in terms of the classifier output) for each science program to define trigger conditions for same night and long-term monitoring. For example, a supernova program may define same night triggers for all objects with at least a 25% chance of being a supernova but no more than a 1% chance of being an asteroid. Discoveries worthy of same-night follow-up will be sent primarily to P60, although sources identified at the end of the night may fall to Faulkes Telescope North (FTN; Haleakala, Hawaii) in rare cases where twilight preempts the required observation. These requests will be issued as ToO triggers, similar to the gamma-ray burst triggers already handled by both P60 and FTN except that interruption of integrations or read outs will not be required.

After completion of an observation, the data must be analyzed to extract the target parameters (e.g., the magnitude and position in photometric data or the spectral classification, redshift, etc., for spectral observations). The responsibility for this data reduction lies with the partner in charge of the instrument, and the high-level data will be sent back to the Marshal. The Marshal will then relay this information back to the classifier to refine the classification, and it will archive the observation in its own database for future use.

6. THE FIRST PTF TRANSIENT DETECTIONS

We conclude with the first results from the PTF survey. PTF's first bona fide transient was detected at $m_{g'} = 18.62 \pm 0.04$ mag on UT 2009 March 2.347 (Kulkarni et al. 2009) after subtraction of a reference template made from PTF images acquired on February 25, 26, and 28 (Fig. 10). The transient,

TABLE 3
OPTICAL TRANSIENTS DISCOVERED DURING PTF COMMISSIONING

Name	R.A. (J2000)	Decl. (J2000)	Date UT 2009	Mag	z	Offset from Host		Spect. Classification
PTF09a	14:23:55.82	+35:11:05.2	Mar 02.3470	18.6	0.06	0.9″ W	2.7″ S	SN Ia
PTF09d	09 15 36.57	+50 34 51.5	Mar 17.1476	19.5				CV
PTF09e	09 14 34.16	+51 10 29.7	Mar 17.1476	20.0	0.15	0.1″ E	0.8″ S	SN Ia
PTF09f	11 41 54.05	+10 25 46.1	Mar 17.1759	20.1	0.15	0.5″ E	2.6″ S	SN Ia
PTF09g	15 16 31.50	+54 27 35.4	Mar 17.2681	18.4	0.04	0.5″ E	4.5″ N	SN II
PTF09h	08 00 47.28	+46 56 53.8	Mar 17.1418	20.2	0.12	0.4″ E	0.4″ S	SN Ia
PTF09k	12 26 17.84	+48 26 49.5	Mar 17.1880	20.9	0.19	5.3″ W	6.3″ N	SN Ia
PTF09o	04 05 02.73	+73 24 54.2	Mar 17.1343	18.5				CV?
PTF09q	12 24 50.17	+08 25 57.6	Mar 17.2195	19.6	0.09	1.8″ E	3.9″ S	SN Ic
PTF09r	14 18 58.68	+35 23 16.1	Mar 17.2572	19.2	0.03	0.7″ E	0.8″ N	SN II
PTF09s	12 06 51.67	+26 57 36.7	Mar 17.1789	17.8	0.05	0.2″ W	0.0″ N	SN Ia
PTF09t	14 15 43.29	+16 11 59.1	Mar 17.2664	18.6	0.04	4.6″ E	1.4″ S	SN II
PTF09u	14 29 39.61	+39 09 32.8	Mar 17.2557	20.0	0.13	0.0″ W	2.0″ N	SN Ia
PTF09v	13 27 10.50	+31 30 32.5	Mar 17.2091	19.2	0.12	0.7″ W	0.5″ N	SN Ia
PTF09x	13 21 45.15	+42 33 06.2	Mar 21.3851	20.2	0.25	0.8″ W	1.2″ N	SN Ia
PTF09y	11 16 34.27	+03 32 02.8	Mar 21.1860	20.1	0.19	0.2″ W	2.1″ N	SN?
PTF09z	11 54 42.23	+55 18 10.7	Mar 21.4275	20.1	0.19	0.1″ W	0.4″ N	SN Ia
PTF09aa	11 33 20.71	−09 24 40.3	Mar 21.1961	19.0	0.12	0.0″ W	0.2″ N	SN Ia
PTF09ab	09 22 15.69	+45 44 53.4	Mar 21.3599	19.5	0.17	0.0″ E	0.1″ N	SN Ia
PTF09ac	12 24 35.31	+47 14 16.8	Mar 21.4350	19.2	0.16	6.1″ W	1.2″ N	SN Ia
PTF09ad	11 03 06.64	+50 09 36.3	Mar 21.4313	19.8	0.20	0.6″ W	1.4″ N	SN Ia
PTF09aj	09 45 30.46	+06 32 25.0	Mar 21.2155	17.8	0.09	0.2″ W	1.5″ N	SN Ia
PTF09as	12 59 15.85	+27 16 41.3	Mar 25.1642	19.1	0.19	1.7″ W	5.5″ N	SN Ia
PTF09av	09 15 12.73	+19 05 46.3	Mar 25.1522	20.2	0.22	2.0″ W	2.9″ S	SN Ia
PTF09aw	14 15 19.36	+16 25 14.0	Mar 25.2625	19.7	0.17	4.7″ W	4.5″ S	SN Ia
PTF09bc	10 51 08.55	+74 05 23.2	Mar 20.2834	20.51	0.18	3.9″ E	1.9″ N	SN Ia
PTF09bd	08 07 29.72	+15 34 41.8	Mar 20.1407	16.9				CV
PTF09be	14 10 18.54	+16 53 38.8	Mar 26.2304	19.0		4.7″ E	3.9″ N	SN II
PTF09bh	12 24 39.20	+08 55 59.2	Mar 28.4155	20.5	0.18	1.6″ W	0.8″ N	SN Ia
PTF09bi	11 46 50.12	+11 47 55.3	Mar 25.1613	19.6	0.11	2.6″ W	0.7″ S	SN II?
PTF09bj	11 18 06.46	+12 53 43.1	Mar 25.1627	18.1	0.14	0.1″ E	1.3″ N	SN Ia
PTF09bw	15 05 01.97	+48 40 03.9	Mar 28.4039	20.3	0.15	0.8″ W	0.7″ N	SN IIn?
PTF09bx	14 30 50.42	+35 37 31.4	Mar 26.2086	18.8		4.2″ E	3.3″ S	SN?
PTF09by	13 29 12.64	+46 43 27.5	Mar 26.2509	19.3	0.10	0.2″ E	0.9″ N	SN Ia
PTF09ct	11 42 13.88	+10 38 54.0	Mar 27.1606	20.3	0.15	5.6″ W	5.2″ N	SN II?
PTF09cu	13 15 23.15	+46 25 09.4	Mar 26.2509	17.9	0.06	7.5″ W	3.9″ S	SN II
PTF09dh	14 44 42.08	+49 43 44.9	Apr 17.375	20.3	0.1			SN
PTF09ds	14 09 16.65	+53 06 13.2	May 15.236	20.6	0.179	0.9″ W	0.2″ N	SN Ia
PTF09ec	13 12 54.49	+43 28 36.0	May 15.259	19.8	0.091	0.3″ E	0.0″ N	SN Ia
PTF09fb	16 46 42.82	+75 15 28.6	May 16.198	17.7	0.042	0.0″ E	0.2″ S	SN Ia
PTF09fr	14 50 00.12	+44 55 05.8	May 17.172	19.1	0.08	2.5″ E	5.6″ N	SN Ia
PTF09fs	17 36 44.28	+53 40 12.3	May 17.244	20.3	0.109	1.4”W	3.5″ S	SN
PTF09&	16 33 10.88	+53 05 30.4	May 17.247	20.5	0.17	8.1″ W	2.5″ N	SN Ia
PTF09go	16 47 34.80	+49 50 00.4	May 17.237	18.1	0.047	0.2″ W	0.2″ S	SN II
PTF09do	17 38 26.04	+53 23 00.4	May 15.220	20.2	0.080	4.0″ E	1.1″ N	SN Ia
PTF09ge	14 57 03.10	+49 36 40.8	May 17.229	19.4	0.064	0.1″ E	0.1″ S	SN?
PTF09gk	15 06 11.06	+53 17 42.9	May 17.253	20.0	0.0			CV
PTF09gm	15 27 48.59	+41 35 34.0	May 17.196	19.4	0.082	0.2″ E	1.6″ S	SN Ia
PTF09gn	15 29 10.95	+40 47 39.0	May 17.196	20.4	0.139	1.1″ W	0.4″ S	SN Ia
PTF09ib	15 44 38.77	+45 47 51.0	May 20.401	20.4	0.123	0.1″ E	0.2″ S	SN Ia
PTF09ij	14 32 14.62	+54 51 19.7	May 20.288	20.3	0.123	3.7″ W	2.1″ N	SN
PTF09jw	12 54 23.74	+56 43 57.5	May 20.245	20.4	0.153	0.2″ E	0.3″ N	SN Ia

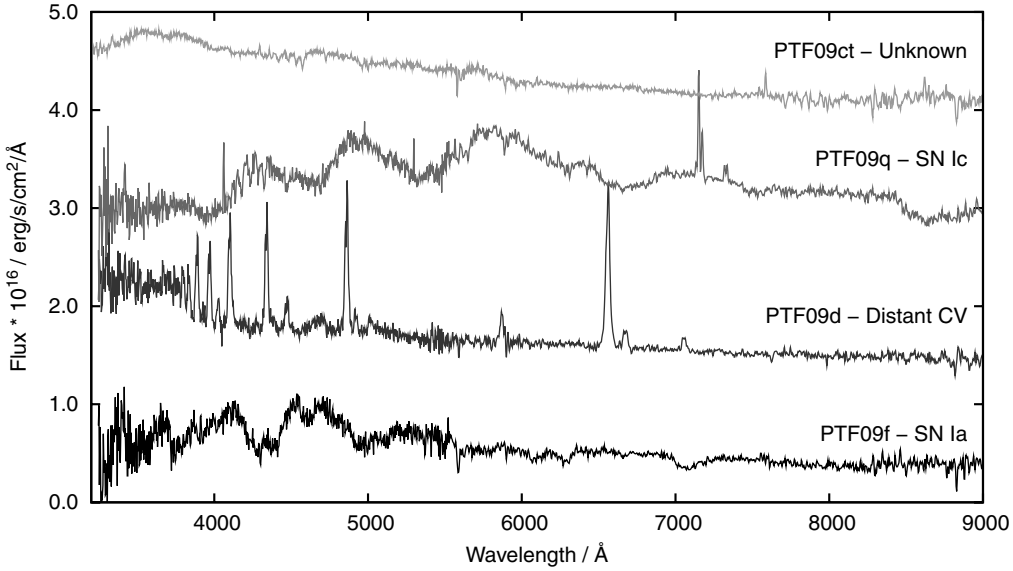

FIG. 11.—Keck LRIS spectra of several different types of optical transients discovered and classified by PTF. Spectra are not redshift corrected, and are vertically offset for clarity. Details of the detected transients can be found in Table 3.

at R.A. $= 14^{\rm h}23^{\rm m}55^{\rm s}82$, decl. $= +35°11'05''.2$ (J2000, uncertainty $<1''$), was offset $0.9''$ W and $2.7''$ S from the core of an SDSS galaxy with $m_g = 17.78$ and a redshift of $z = 0.0555$.

We obtained spectra of the transient on March 8.388 UT with the Double Beam Spectrograph (DBSP) instrument on the 5.1 m Palomar Hale telescope. The transient turned out to be a normal Type-Ia supernova at a redshift consistent with the apparent SDSS host. In this restframe, the expansion velocity derived from the minimum of the Si II (rest 635.5 nm) line was about $10,700$ km s^{-1}. The best match found with the Superfit SN spectral identification code (Howell et al. 2005) was to SN 1994D at 8 days prior to maximum light.

During the commissioning process many further transients have been detected and followed up (Table 3; Fig. 11). Eleven were detected during an R-band search of 498 square degrees (Kasliwal et al. 2009b), using reference images acquired by PTF prior to March 12. All 11 transients were spectroscopically classified on UT 2009 March 20 using DBSP. Twenty-five optical transients were found in a search of several nights of commissioning data taken between March 17 and March 28, photometrically followed up with P60, and spectroscopically classified using the Hale, Hobby-Eberly, and Keck telescopes (Quimby et al. 2009a). A very bright supernova was detected on April 17 (Quimby et al. 2009b) and a further 15 optical transients were discovered and followed up in 2009 May (Kasliwal et al. 2009a). These detections represent a small fraction of the ultimate PTF discovery power, as the majority of the commissioning time was used for acquiring reference images.

These initial transient detections have opened the Palomar Transient Factory for business. The full PTF survey started in 2009 June and the project is scheduled to continue until at least the end of 2012.

This paper is based on observations obtained with the Samuel Oschin Telescope and the 60 inch Telescope at the Palomar Observatory as part of the Palomar Transient Factory project, a scientific collaboration between the California Institute of Technology, Columbia University, Las Cumbres Observatory, the Lawrence Berkeley National Laboratory, the National Energy Research Scientific Computing Center, the University of Oxford, and the Weizmann Institute of Science. S. R. K. and his group were partially supported by the NSF grant AST-0507734. J. S. B. and his group were partially supported by a Hellman Family Grant, a Sloan Foundation Fellowship, NSF/DDDAS-TNRP grant CNS-0540352, and a continuing grant from DOE/SciDAC. T. B., A. P., W. R. and D. A. H. are supported by the TABASGO foundation and the Las Cumbres Observatory Global Telescope Network. The Weizmann Institute PTF partnership is supported by an ISF equipment grant to A. G. A. G.'s activity is further supported by a Marie Curie IRG grant from the EU, and by the Minerva Foundation, Benoziyo Center for Astrophysics, a research grant from Peter and Patricia Gruber Awards, and the William Z. and Eda Bess Novick New Scientists Fund at the Weizmann Institute. E. O. O. acknowledges partial support from NASA through grants HST-GO-11104.01-A; NNX08AM04G; 07-GLAST1-0023; and HST-AR-11766.01-A. A. V. F. and his group are grateful for funding from NSF grant AST–0607485, DOE/SciDAC grant DE-FC02-06ER41453, DOE grant DE-FG02-08ER41563, the TABASGO Foundation, Gary and Cynthia Bengier, and the Sylvia and Jim Katzman Foundation.

S. G. D. and A. A. M. were supported in part by NSF grants AST-0407448 and CNS-0540369, and also by the Ajax Foundation. The National Energy Research Scientific Computing Center, which is supported by the Office of Science of the U.S. Department of Energy under Contract No. DE-AC02-05CH11231, has provided resources for this project by supporting staff and providing computational resources and data storage. A. V. F. and his group are grateful for funding from NSF grant AST–0607485, DOE/SciDAC grant DE-FC02-06ER41453, DOE grant DE-FG02-08ER41563, the TABASGO Foundation, Gary and Cynthia Bengier, the Richard and Rhoda Goldman Fund, and the Sylvia and Jim Katzman Foundation. L. B.'s research is supported by the NSF via grants PHY 05-51164 and AST 07-07633. M. S. acknowledges support from the Royal Society and the University of Oxford Fell Fund.

REFERENCES

Aldering, G., Adam, G., Antilogus, P., Astier, P., Bacon, R., Bongard, S., Bonnaud, C., Copin, Y., et al. 2002, Proc. SPIE, 4836, 61

Ashe, M. C., Bonati, M., & Heathcote, S. 2002, Proc. SPIE, 4848, 508

Bambery, R., Helin, E. F., Pravdo, S. H., Hicks, M., Lawrence, K. J., Thicksten, R., Brown, M., Kuluhiwa, K., & et al. 2007, Minor Planet Circ., 5958, 1

Bertin, E. 2006, in ASP Conf. Ser. 351, Astronomical Data Analysis Software and Systems XV, ed. C. Gabriel, C. Arviset, D. Ponz, & S. Enrique, 112

Bertin, E., & Arnouts, S. 1996, A&AS, 117, 393

Bloom, J. S., Starr, D. L., Butler, N. R., Nugent, P., Rischard, M., Eads, D., & Poznanski, D. 2008, Astron. Nachr., 329, 284

Cenko, S. B., Fox, D. B., Moon, D.-S., Harrison, F. A., Kulkarni, S. R., Henning, J. R., Guzman, C. D., Bonati, M., et al. 2006, PASP, 118, 1396

Cuillandre, J.-C., Luppino, G. A., Starr, B. M., & Isani, S. 2000, Proc. SPIE, 4008, 1010

Djorgovski, S. G., Baltay, C., Mahabal, A. A., Drake, A. J., Williams, R., Rabinowitz, D., Graham, M. J., Donalek, C., et al. 2008, Astron. Nachr., 329, 263

Harrington, R. G. 1952, PASP, 64, 275

Howell, D. A., Sullivan, M., Perrett, K., Bronder, T. J., Hook, I. M., Astier, P., Aubourg, E., Balam, D., et al. 2005, ApJ, 634, 1190

Kasliwal, M. M., Kulkarni, S. R., Quimby, R., Nugent, P., Howell, D. A., Cooke, J., Cenko, S., Gal-Yam, A., et al. 2009a, ATel, 2055, 1

Kasliwal, M. M., Quimby, R., Nugent, P., Ellis, R. S., Howell, A., Kulkarni, S. R., Law, N., Ofek, E. O., et al. 2009b, ATel, 1983, 1

Krisciunas, K., & Schaefer, B. E. 1991, PASP, 103, 1033

Kulkarni, S. R., Law, N. M., Quimby, R., Kasliwal, M., et al. 2009, ATel, 1964, 1

Mahabal, A., Djorgovski, S. G., Turmon, M., Jewell, J., Williams, R. R., Drake, A. J., Graham, M. G., Donalek, C., et al. 2008a, Astron. Nachr., 329, 288

Mahabal, A., Djorgovski, S. G., Williams, R., Drake, A., Donalek, C., Graham, M., Moghaddam, B., Turmon, M., et al. 2008b, in AIP Conf. Ser. 1082, 287–293

Monet, D. G., Levine, S. E., Canzian, B., Ables, H. D., Bird, A. R., Dahn, C. C., Guetter, H. H., Harris, H. C., et al. 2003, AJ, 125, 984

Ofek, E. O. 2008, PASP, 120, 1128

Parker, Q. A., & Bland-Hawthorn, J. 1998, PASA, 15, 33

Perlmutter, S., Aldering, G., Goldhaber, G., Knop, R. A., Nugent, P., Castro, P. G., Deustua, S., Fabbro, S., et al. 1999, ApJ, 517, 565

Quimby, R., Kasliwal, M. M., Cenko, S. B., Fox, D., Gal-Yam, A., Howell, D. A., Kulkarni, S. R., Law, N., 2009a, ATel, 2005, 1

Quimby, R., Kasliwal, M. M., Nugent, P., Howell, D. A., Rau, A., & Bhalerao, V. 2009b, ATel, 2037, 1

Rahmer, G., Smith, R., Velur, V., Hale, D., Law, N., Bui, K., Petrie, H., & Dekany, R. 2008, Proc. SPIE, 7014

Rau, A., Kulkarni, S., Law, N., Bloom, J., & Ciardi, D., et al. 2009, PASP, 121, 1334

Reid, I. N., Brewer, C., Brucato, R. J., McKinley, W. R., Maury, A., Mendenhall, D., Mould, J. R., Mueller, J., et al. 1991, PASP, 103, 661

Starr, D. L., Bloom, J. S., & Butler, N. R. 2008a, in ASP Conf. Ser. 394, Astronomical Data Analysis Software and Systems XVII, ed. R. W. Argyle, P. S. Bunclark, & J. R. Lewis, 609

———. 2008b, in AIP Conf. Ser. 1000, ed. M. Galassi, D. Palmer, & E. Fenimore, 635

York, D. G., Adelman, J., Anderson, J. E., Jr., Anderson, S. F., Annis, J., Bahcall, N. A., & Bakken, J. A. 2000, AJ, 120, 1579